IOPscience iopscience.iop.org

Home Search Collections Journals About Contact us My IOPscience

Structural, electronic and vibrational properties of small Ga_xN_y ($x+y = 2–5$) nanoclusters: a B3LYP-DFT study

This article has been downloaded from IOPscience. Please scroll down to see the full text article.

2007 J. Phys.: Condens. Matter 19 076209

(http://iopscience.iop.org/0953-8984/19/7/076209)

View the table of contents for this issue, or go to the journal homepage for more

Download details:
IP Address: 129.252.86.83
The article was downloaded on 28/05/2010 at 16:07

Please note that terms and conditions apply.

IOP PUBLISHING JOURNAL OF PHYSICS: CONDENSED MATTER

J. Phys.: Condens. Matter **19** (2007) 076209 (28pp) doi:10.1088/0953-8984/19/7/076209

Structural, electronic and vibrational properties of small Ga_xN_y ($x + y = 2$–5) nanoclusters: a B3LYP-DFT study

P S Yadav, R K Yadav and B K Agrawal

Physics Department, Allahabad University, Allahabad-211002, India

E-mail: phsyadav@rediffmail.com

Received 7 November 2006, in final form 1 January 2007
Published 2 February 2007
Online at stacks.iop.org/JPhysCM/19/076209

Abstract

An *ab initio* study of the stability, structural and electronic properties has been made for 49 gallium nitride nanoclusters, Ga_xN_y ($x + y = 2$–5). Among the various configurations corresponding to a fixed $x + y = n$ value, the configuration possessing the maximum value of binding energy (BE) is named as the most stable structure. The vibrational and optical properties have been investigated only for the most stable structures. A B3LYP-DFT/6-311G(3df) method has been employed to optimize the geometries of the nanoclusters fully. The binding energies (BEs), highest-occupied and lowest-unoccupied molecular orbital (HOMO–LUMO) gaps and the bond lengths have been obtained for all the clusters. We have considered the zero-point energy (ZPE) corrections ignored by the earlier workers. The adiabatic and vertical ionization potentials (IPs) and electron affinities (EAs), charge on atoms, dipole moments, vibrational frequencies, infrared intensities (IR Int.), relative infrared intensities (Rel. IR Int.) and Raman scattering activities have been investigated for the most stable structures. The configurations containing the N atoms in majority are seen to be the most stable structures. The strong N–N bond has an important role in stabilizing the clusters. For clusters containing one Ga atom and all the others as N atoms, the BE increases monotonically with the number of the N atoms. The HOMO–LUMO gap and IP fluctuate with the cluster size n, having larger values for the clusters containing odd number of N atoms. On the other hand, the EA decreases with the cluster size up to $n = 3$, and shows slow fluctuations thereafter for the larger clusters. In general, the adiabatic IP (EA) is smaller (greater) than the vertical IP (EA) because of the lower energies of the most stable ground state of the cationic (anionic) clusters. The optical absorption spectrum or electron energy loss spectrum (EELS) is unique for every cluster, and may be used to characterize a specific cluster. All the predicted physical quantities are in good agreement with the experimental data wherever available. The growth of these most stable structures should be possible in experiments.

(Some figures in this article are in colour only in the electronic version)

 © 2007 IOP Publishing Ltd Printed in the UK

1. Introduction

Recently, group III nitrides and their alloys which possess wide band gaps have drawn great attention for their applications in light-emitting devices in the blue–green spectral region and also as high-temperature, high-power electronics [1–3]. An understanding of the physical properties of these clusters at the atomic level is required for their possible applications in microelectronic devices. A number of theoretical and experimental studies on the physical properties of both the surfaces and the bulk have been undertaken. However, a study of the small-size clusters of these nitrides is still lacking.

An exciting phase in between the molecule and solid is an atomic cluster, whose electronic and other properties may be exotic [4, 5]. In clusters, the high surface area to volume ratio is quite high as compared to the bulk [6, 7]. The sizes of the electronic devices have been reduced because of this advancement.

For the preparation of devices, GaN nanoclusters may be prepared by using sequential ion implantation in a dielectric matrix [8]. There have been very few experimental investigations on GaN nanoclusters. Experiments have been done on the organometallic precursors for the chemical vapour deposition process of GaN heterostructures [9]. The emergence of nanotechnology has driven the building of smaller electrical and optical devices based on nanostructures such as nanotubes and nanowires. Some devices like FETs [10] and nanoscale lasers [11] have been fabricated which are based on a single GaN wire. As devices become even smaller and the confinement effects become more prominent, it is hoped that a study of the electrical properties of small clusters of GaN will lead to a better understanding of the properties of such devices. Photoelectron (PE) spectroscopy of anions is an ideal technique to study the small clusters due to its mass selectivity and because it provides information on the structures and energetics of the neutral clusters [12].

Some experimental studies have been done on GaN clusters. Zhou and Andrews [13] have performed both experimental and theoretical studies of Ga_mN_n ($m+n = 2$–4) clusters by using laser ablation and the infrared matrix isolation technique and the density functional theory (DFT) method. Matrix isolation experiments were also performed by Himmel *et al* [14] to study the interaction between Ga atoms and N_2 by using Raman and UV/vis spectroscopies for detection and analysis. More recently, Sheehan *et al* [15] have measured anion photoelectron spectra of Ga_2N^- and the vibrational spectra of Ga_2N.

Kandalam and co-workers [16–19] have performed a first-principles study of both nonstoichiometric and stoichiometric GaN clusters. The same group has also studied stoichiometric Ga_nN_n ($n = 3$–6) [17, 18] clusters and investigated nonstoichiometric Ga_mN_2 ($m = 2$–6) clusters [19]. Belbruno [20] studied the geometrical and electronic structures of stoichiometric Ga_nN_n ($n = 2$–4) clusters using density functional theory. Costales and Pandey [21] computed the electronic structures of small Ga_nN_n ($n = 1$–3) anionic clusters using density functional calculations. Song *et al* [22–26] employed the full potential linear-muffin-tin-orbital molecular dynamics (FPLMTO-MD) method to study both nonstoichiometric and stoichiometric GaN clusters. Wang and Balasubramanian [27] have investigated the low-lying electronic states of Ga_2N, GaN_2, and the corresponding anions and cations. Very recently, Song *et al* [28] have studied Ga_nN ($n = 1$–19) clusters using DFT with a generalized gradient approximation (GGA). For Ga_xN_y ($x + y = 2$–5) clusters, the required physical properties such as IP, EA vibrational frequencies, IR intensities and Raman scattering activities for all the possible configurations have not been reported.

The usual local density approximation (LDA) theory has been seen to be quite successful in predicting the ground-state properties of the various types of system, for example clusters, wires, surfaces and bulks. In general, the excited states are seen to be unreliable, which leads

to the occurrence of the underestimation of the electron energy gap. An extension of this static density functional theory, namely the time-dependent linear response formalism of the DFT (TDDFT), has recently been employed for an efficient calculation of the excited-state properties.

In the present paper, we report on a theoretical study of the equilibrium geometries, stability, structural, highest-occupied and lowest-unoccupied molecular orbital (HOMO–LUMO) gap, adiabatic and vertical ionization potential (IP) and electron affinity (EA), charge on atoms, dipole moment, and vibrational, optical and Raman scattering activities of small Ga_xN_y ($x + y = 2$–5) nanoclusters by using the B3LYP-DFT/6-311G(3df) method. For the investigation of the optical properties, we employed the TDDFT formalism [29–35]. In section 2, we present the method used in the computation. Section 3 contains the calculation and results. The conclusions are contained in section 4.

2. Method

One makes a linear combination of Gaussian functions to obtain the atomic orbitals, which are also called the contracted functions. A large basis set for each atom is selected for a precise calculation. We use the triple split valence basis set, 6-311G, where one employes three sizes of the contracted functions per orbital type. The advantage of the split valiance basis set is that it allows the orbitals to change their size without making any change in the shape of the orbitals. For overcoming this limitation, one uses a polarizable basis set 6-311G(3df) by adding orbitals with the angular momentum beyond what is necessary for the description of the ground state of each atom. For N and Ga atoms we add three d functions and one f function respectively. For generating the quite accurate structural parameters one uses the triple zeta basis set and the multiple polarization functions.

The exact exchange in the Hartree–Fock theory for a single determinant is replaced in the DFT by a more general expression, the exchange–correlation functional, which can include terms accounting both for the exchange energy and the electron correlation.

In BLYP, one considers the Becke [36] exchange functional and the correlation function of Lee, Yang and Parr (LYP) [37, 38] which includes both local and nonlocal contribution. In B3LYP, we employ the three parameter hybrid functionals of Becke [36]. It may be noted that the Becke functional considers the Slater exchange along with the corrections involving the gradient of the density [36].

For the optimization of the GaN clusters, we have employed the B3LYP-DFT/6-311G(3df) version in the Gaussian-03 code [39] which employes the hierarchy of procedures corresponding to different approximation methods. The usual TDDFT formalisms have been considered for calculating the optical spectra.

3. Calculation and results

3.1. Stability of structures

Different types of structure, including linear chains, rings, planar and three-dimensional ones, have been investigated. The minimum energy for each structure is achieved by relaxing the atomic positions. Convergence in the system energy up to 10^{-3} meV and forces of 10^{-3} eV $Å^{-1}$ on each atom were achieved.

In order to have stability, we define the binding energy of the cluster. We subtract the total energy of the cluster from the sum of the energies of all the isolated atoms present in the cluster and divide the resultant quantity by the number of atoms. We name this as the binding energy

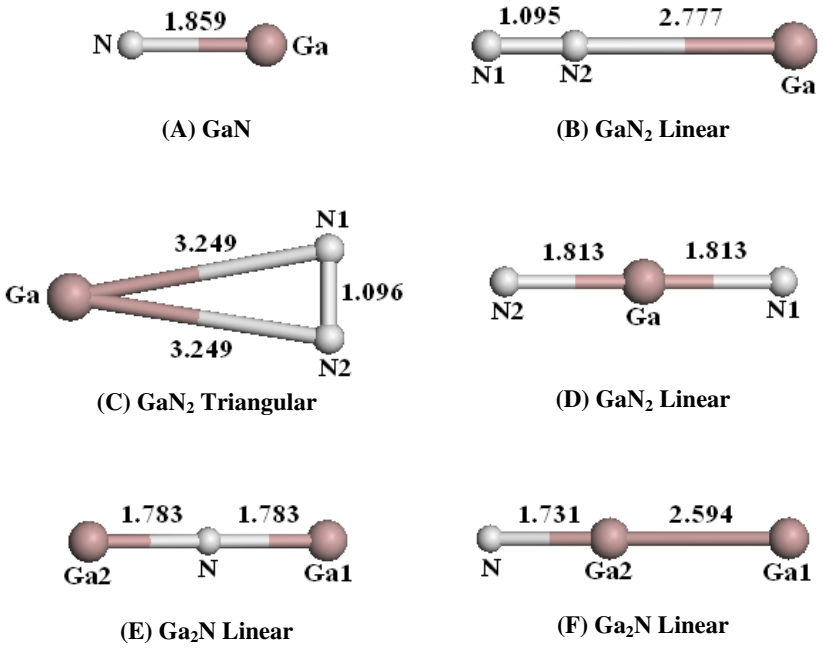

Figure 1. Optimized structures of GaN (A), GaN_2, and Ga_2N nanoclusters. For GaN_2, there are three configurations: linear GaNN (B), triangular GaN_2 (C), and linear NGaN (D). For Ga_2N, there are two configurations: linear GaNGa (E) and linear GaGaN (F).

(BE) per atom. For a more precise calculation, we have calculated the harmonic vibrational frequencies and the corresponding zero point energies (ZPEs) have been subtracted from the earlier calculated BE values so that our final binding energy (FBE) = BE − ZPE. Among all the complexes pertaining to a specific chemical formula Ga_xN_y, the configuration possessing the maximum value of BE is named as the most stable structure.

We present all the 49 optimized structures in figures 1–7. The computed N–N, Ga–N and Ga–Ga bond lengths are 1.09, 1.86 and 2.48 Å, respectively. The calculated N–N and Ga–Ga bond lengths are in excellent agreement with the experimental values [40], 1.10 and 2.44 Å. The corresponding bond energies are 9.99, 2.29 and 1.19 eV, respectively, which are again in very close agreement with the experimental values [40], 9.81 and 1.43 eV. One may expect the minimum energies for those complexes which contain the maximum number of N–N bonds, followed by Ga–N and Ga–Ga bonds.

The symmetry, multiplicity of the ground state and the BEs are given for all the optimized structures in table 1. The BEs reported by other workers have also been included for comparison. The most stable structures have been depicted in bold letters in table 1. During the optimization for each structure, we have selected the ground state with minimum energy, and the multiplicity of the ground state has been shown in table 1. For the most stable structures, the calculated N–N, Ga–N and Ga–Ga bond lengths are compared with other values in table 2.

A perusal of table 1 reveals that in all the studied nanoclusters the FPLMTO-MD values for the BEs are much higher than those of the present study and the other workers using other methods. Our values for the various structures are also lower than the values reported by other workers using other methods.

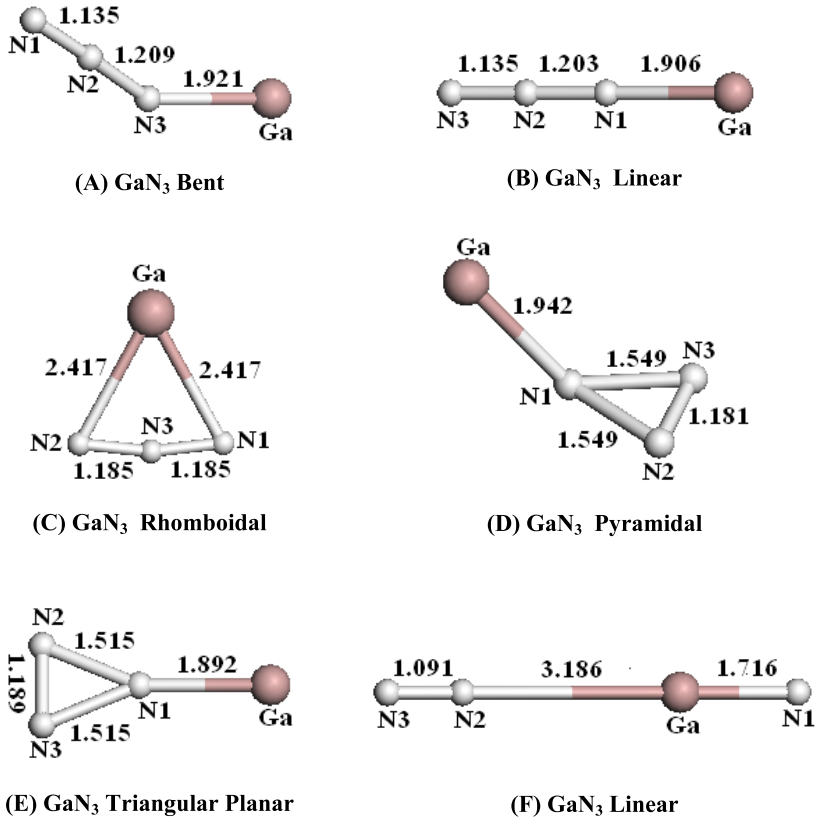

Figure 2. Optimized structures of GaN_3 nanoclusters. There are six different configurations: bent (A), linear GaNNN (B), rhomboidal (C), pyramidal (D), triangular planar (E), and linear NGaNN (F).

We now discuss each cluster individually in the following.

GaN: The ground state of GaN cluster is a triplet state and the singlet state lies above it at 1.26 eV.

The present FBE (1.11 eV) is slightly lower than the values of other workers [16, 21, 26, 28] who have not considered the ZPE in their estimate. No experimental data are available for comparison. Our value for Ga–N bond length (1.86 Å) is smaller as compared to other values [13, 16, 20, 28, 41].

Ga_xN_y ($x + y = 3$): The ground states of all the linear and triangular structures are doublets, except the NGaN linear structure, which possesses the quartet ground state.

GaN_2: We have considered two linear configurations and a triangular configuration. Among them, the linear GaNN and the triangular structures have maximum and quite similar FBEs (3.20 and 3.19 eV, respectively). Wang and Balasubramanian [27] have reported linear GaNN as the lowest-energy structure. These results are in sharp disagreement with the conclusion of Zhou and Andrews [13] that linear NGaN is the lowest-energy structure. For the linear

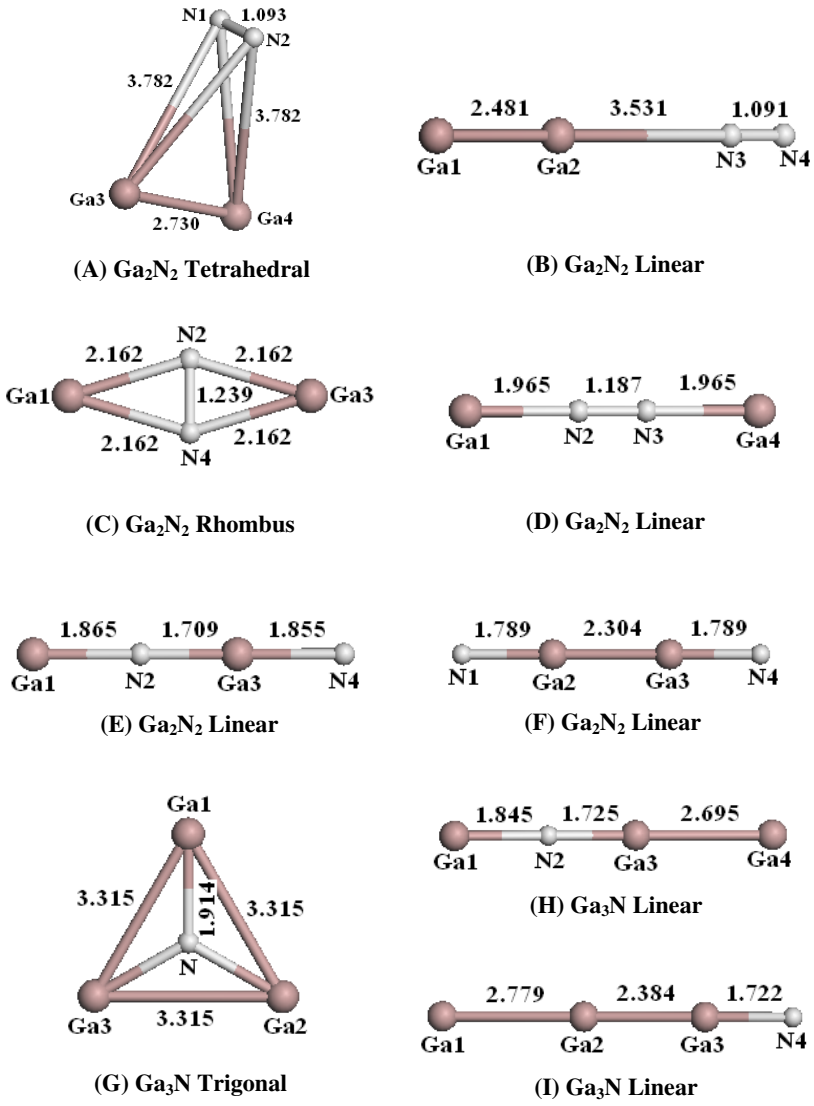

Figure 3. Optimized structures of Ga_2N_2 and Ga_3N nanoclusters. For Ga_2N_2, there are six configurations: tetrahedral (A), linear GaGaNN (B), rhomboidal (C), linear GaNNGa (D), linear GaNGaN (E), and linear NGaGaN (F). For Ga_3N, there are three configurations: trigonal (G), linear GaNGaGa (H), and linear GaGaGaN (I).

(GaNN) structure, the present Ga–N (N–N) bond lengths are larger (smaller) than those reported by other workers [16, 27]. The same is true for the triangular structure. The presently calculated bond angle N_1GaN_2 of 19° is smaller than that 26° of Kandalam *et al* [16] and 33° of Song *et al* [26].

Ga_2N: Here, the investigated configurations are similar to GaN_2. The triangular structure was found to be unstable. Among the remaining ones, the linear GaNGa structure is the lowest-energy structure. A similar conclusion has also been reported by earlier workers [15, 27, 28].

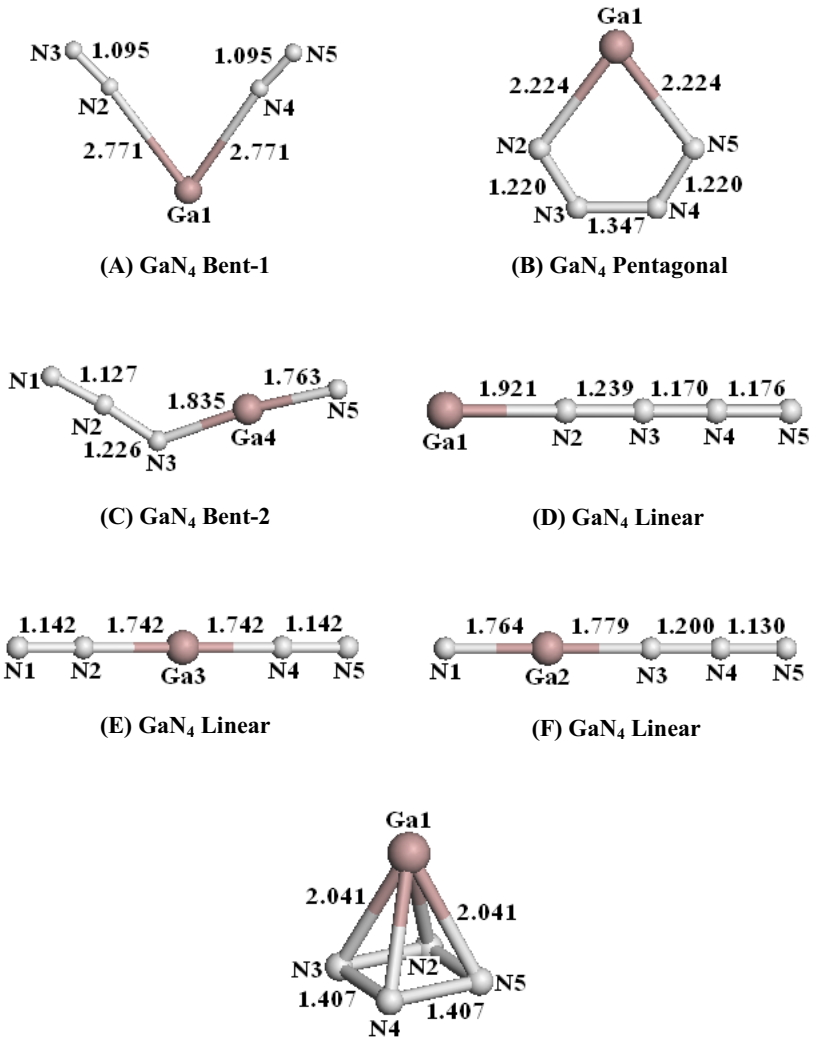

(A) GaN_4 Bent-1 **(B) GaN_4 Pentagonal**

(C) GaN_4 Bent-2 **(D) GaN_4 Linear**

(E) GaN_4 Linear **(F) GaN_4 Linear**

(G) GaN_4 Pyramidal

Figure 4. Optimized structures of GaN_4 nanoclusters. There are seven different configurations: bent-1 (A), pentagonal (B), bent-2 (C), linear GaNNNN (D), linear NNGaNN (E), linear NGaNNN (F), and pyramidal (G).

Our computed Ga–N bond length (1.78 Å) is surprisingly the same as that reported by other workers [13, 15, 16, 27, 28].

Ga_xN_y ($x + y = 4$): All the four atom structures have singlet ground states except Ga_2N_2, where both singlet and triplet states are seen to be the lowest-energy ground states.

GaN_3: We have investigated six different configurations: two linear chains (GaNNN and NGaNN), bent, rhomboidal, triangular planar and triangular pyramidal ones. The bent and linear GaNNN geometries have quite similar FBEs, 3.27 eV, but the linear GaNNN geometry

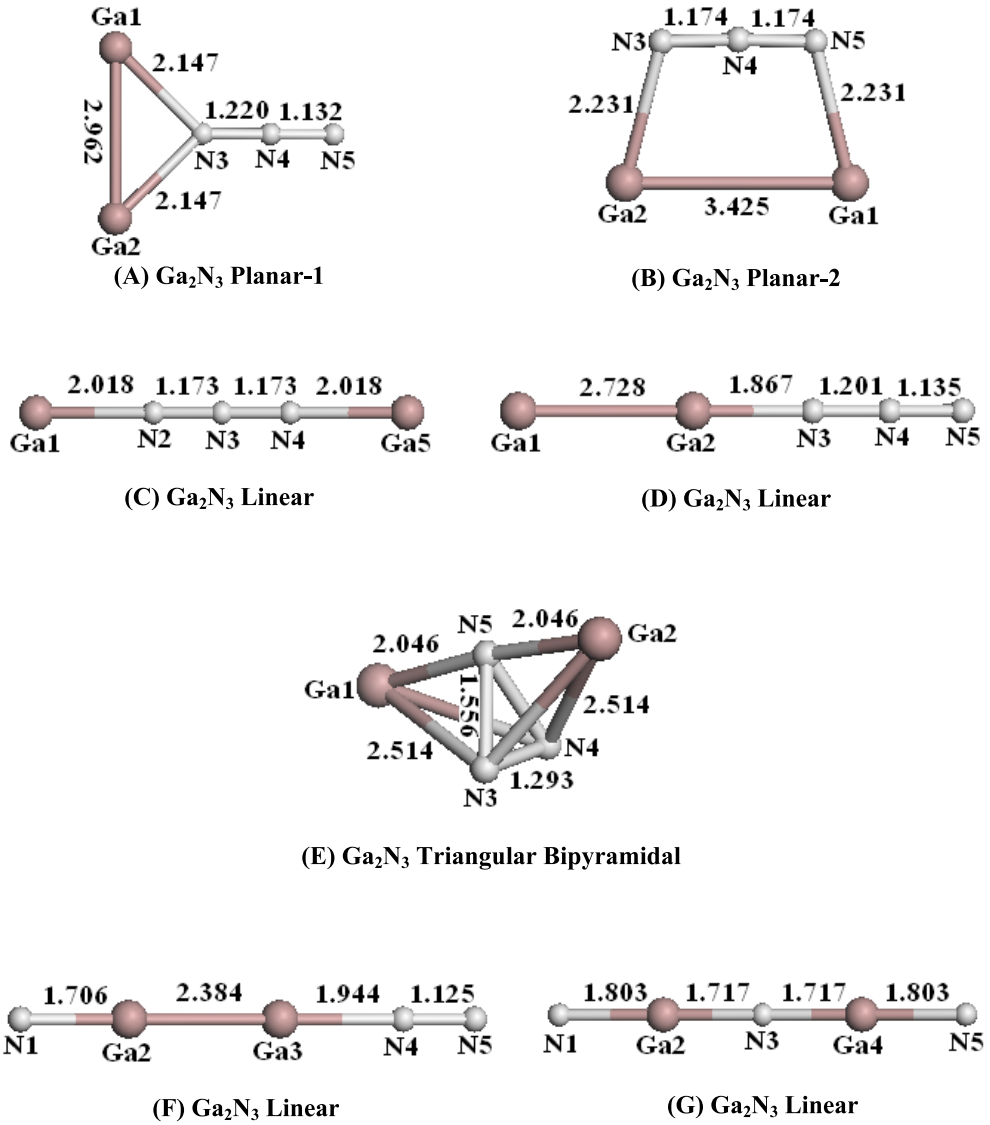

(A) Ga_2N_3 Planar-1 **(B) Ga_2N_3 Planar-2**

(C) Ga_2N_3 Linear **(D) Ga_2N_3 Linear**

(E) Ga_2N_3 Triangular Bipyramidal

(F) Ga_2N_3 Linear **(G) Ga_2N_3 Linear**

Figure 5. Optimized structures of Ga_2N_3 nanoclusters. There are seven different configurations: planar-1 (A), planar-2 (B), linear GaNNNGa (C), linear GaGaNNN (D), triangular bipyramidal (E), linear NGaGaNN (F), and linear NGaNGaN (G).

is unstable due to one imaginary frequency, as will be seen later. Song *et al* [26] have also reported the bent structure to be the most stable. However, their BE is more than double the present value. For the bent structure, the different bond lengths are quite near to those of others [13, 42], and are identical in the majority of cases. Our calculated bond angle GaN_3N_2 (146.6°) agrees well with the Zhou and Andrews [13] angle of 149.5°.

Ga_2N_2: We have studied four linear chains (GaGaNN, GaNNGa, GaNGaN and NGaGaN), a planar rhombus and a tetrahedral configuration. Four of the six studied structures have quite

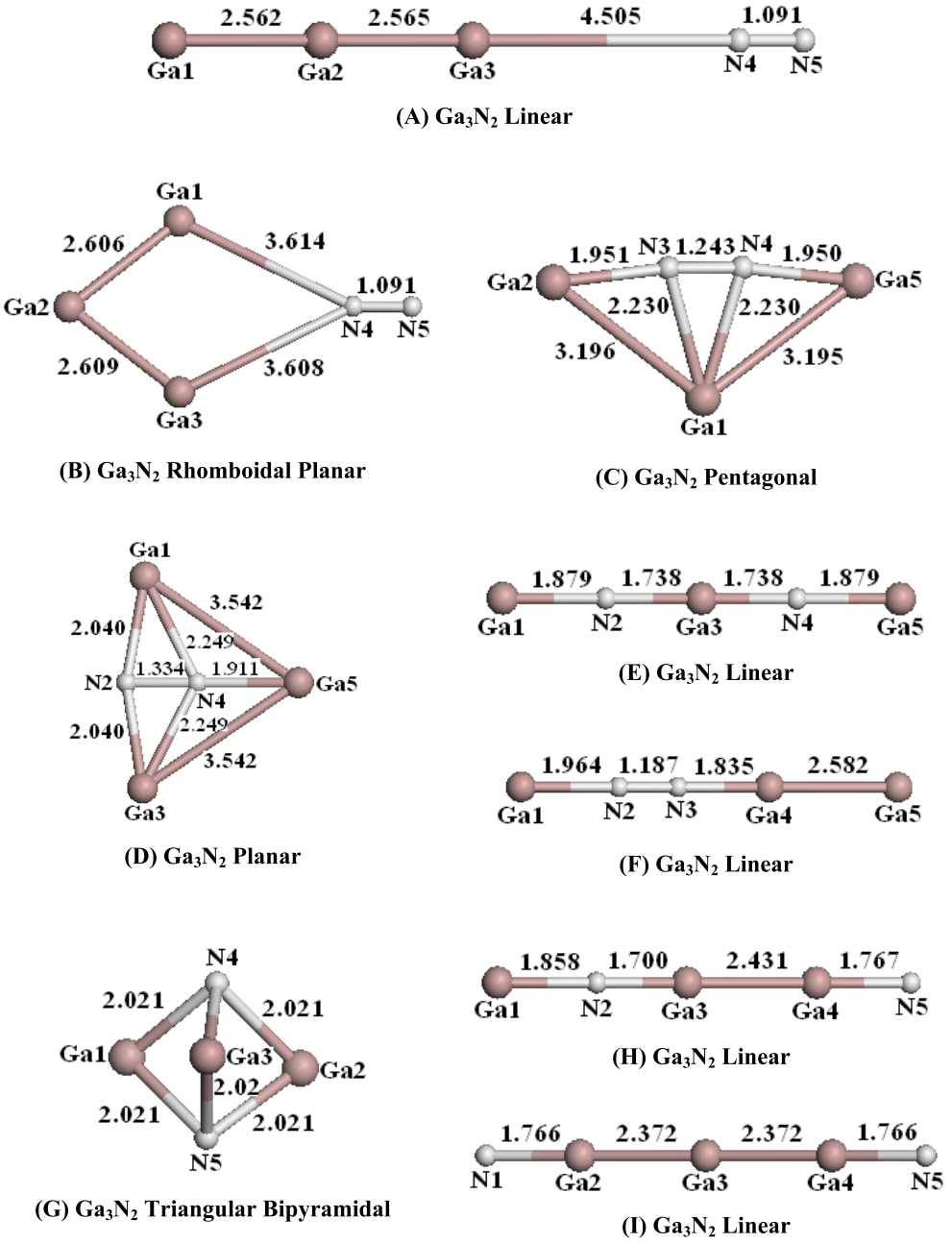

Figure 6. Optimized structures of Ga_3N_2 nanoclusters. There are nine different configurations: linear GaGaGaNN (A), rhomboidal planar (B), pentagonal (C), planar (D), linear GaNGaNGa (E), linear GaNNGaGa (F), triangular bipyramidal (G), linear GaNGaGaN (H), and linear NGaGaGaN (I).

similar and high FBEs. Among them, two structures (tetrahedral and linear GaGaNN) show imaginary vibrational frequency and are thus unstable. The rhombus and the linear GaNNGa

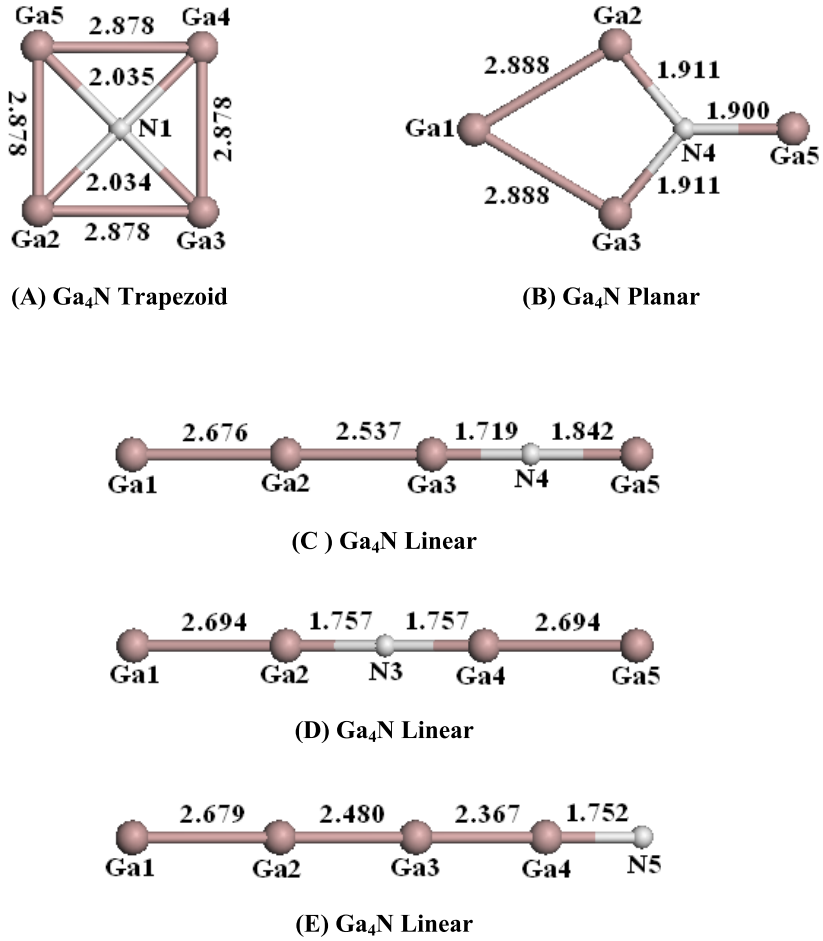

Figure 7. Optimized structures of Ga_4N nanoclusters. There are five different configurations: trapezoid (A), planar (B), linear GaGaGaNGa (C), linear GaGaNGaGa (D), and linear GaGaGaGaN (E).

structures are found to be the most stable structures. The same conclusions have also been reported by Coastales and Pandey [21]. On the other hand, Kandalam *et al* [16] have obtained an imaginary frequency for the linear GaNNGa structure and concluded that the structure is unstable. Their finding is in contrast to the present and other conclusions. Other workers have also reported similar bond lengths for the two stable structures. For the rhombus, our calculated bond angle NGaN (33°) agrees with the value given by Kandalam *et al* [16] (34°).

Ga_3N: We have considered six different geometries, but the trigonal, and two linear (GaGaGaN and GaGaNGa) structures are found to be stable. Among them, the trigonal structure is the most stable one. This conclusion is also reported by earlier workers [26, 28, 42]. Our calculated bond lengths are similar to those reported by earlier workers [26, 28, 42].

Ga_xN_y $(x + y = 5)$: The majority of the structures possess a doubly degenerate ground state.

GaN_4: Seven different geometries were considered, as shown in figure 4. Among them, the bent-1 (4A) is the most stable structure. Song and Cao [26] also reported the same structure as

Table 1. Symmetry, multiplicity of the ground state, binding energy (BE) per atom and HOMO–LUMO gap in eV for all the configurations of Ga_xN_y ($x + y = 2$–5) clusters. The most stable configurations are bold-faced ones. The final binding energy (FBE) = BE − zero point energy (ZPE).

Cluster	Configuration	Symmetry	Multiplicity of the ground state	BE without zero point energy (eV)	Zero point energy (eV)	FBE (eV)		HOMO–LUMO gap (eV)	
						Present	Others	Present	Others
GaN	**Linear Ga–N (1A)**	**$C_{\infty v}$**	**3**	**1.15**	**0.04**	**1.11**	1.12[a] 1.28[b] 1.23[c] 2.76[d]	**2.45**	0.6[b] 3.68[a] 3.94[d]
GaN_2	**Linear GaNN (1B)**	**$C_{\infty v}$**	**2**	**3.36**	**0.16**	**3.20**		**1.35**	
	Triangular (1C)	**C_{2v}**	**2**	**3.35**	**0.16**	**3.19**	6.35[d]	**1.48**	1.01[d]
	Linear NGaN (1D)	$D_{\infty h}$	4	1.34				1.65	
Ga_2N	**Linear GaNGa (1E)**	**$D_{\infty h}$**	**2**	**2.13**	**0.08**	**2.05**	2.30[b]	**2.11**	0.83[b]
	Linear GaGaN (1F)	$C_{\infty v}$	2	1.11				1.41	
GaN_3	**Bent (2A)**	**C_s**	**1**	**3.60**	**0.33**	**3.27**	7.30[d]	**4.98**	
	Linear GaNNN (2B)	$C_{\infty v}$	1	3.60	0.33	3.27		5.29	
	Rhomboidal (2C)	C_{2v}	1	3.38				4.10	
	Pyramidal (2D)	C_s	1	2.87				3.88	
	Triangular planar (2E)	C_{2v}	1	2.86				4.31	
	Linear NGaNN (2F)	$C_{\infty v}$	1	2.78				1.73	
Ga_2N_2	Tetrahedral (3A)	C_{2v}	3	2.84	0.17	2.67		1.34	
	Linear GaGaNN (3B)	$C_{\infty v}$	3	2.81	0.17	2.64		1.28	
	Rhombus (3C)	**D_{2h}**	**1**	**2.79**	**0.18**	**2.61**		**3.32**	
	Linear GaNNGa (3D)	**$D_{\infty h}$**	**3**	**2.78**	**0.18**	**2.60**		**2.14**	1.69[a]
	Linear GaNGaN (3E)	$C_{\infty v}$	3	2.07				2.30	
	Linear NGaGaN (3F)	$D_{\infty h}$	3	1.35				1.53	
Ga_3N	**Trigonal (3G)**	**D_{3h}**	**1**	**2.50**	**0.12**	**2.38**	2.64[b] 3.81[d]	**4.02**	2.87[b] 2.99[d]
	Linear GaNGaGa (3H)	$C_{\infty v}$	1	2.06				2.09	
	Linear GaGaGaN (3I)	$C_{\infty v}$	1	1.14				1.38	
GaN_4	**Bent-1 (4A)**	**C_{2v}**	**2**	**4.03**	**0.32**	**3.71**	7.78[d]	**1.77**	0.60[d]
	Pentagonal (4B)	C_{2v}	4	3.13				1.97	
	Bent-2 (4C)	C_S	2	3.06			6.98[d]	2.52	
	Linear GaNNNN (4D)	$C_{\infty v}$	2	3.06				1.82	
	Linear NNGaNN (4E)	$D_{\infty h}$	2	3.01				1.44	
	Linear NGaNNN (4F)	$C_{\infty v}$	2	3.01				2.45	
	Pyramidal (4G)	C4v	2	2.71			6.96[d]	1.36	

the lowest energy one. Our computed FBE is much lower than the value of Song and Cao [26]. Our Ga–N_2 (N_4) bond length is larger as compared to that of earlier work [26], whereas the

Table 1. (Continued.)

Cluster	Configuration	Symmetry	Multiplicity of the ground state	BE without zero point energy (eV)	Zero point energy (eV)	FBE (eV)		HOMO–LUMO gap (eV)	
						Present	Others	Present	Others
Ga_2N_3	**Planar-1 (5A)**	**C_{2v}**	**2**	**3.09**	**0.35**	**2.74**	6.02[d]	**1.78**	0.31[d]
	Planar-2 (5B)	**C_{2v}**	**2**	**3.03**	**0.34**	**2.69**	5.94[d]	**1.56**	
	Linear GaNNNGa (5C)	$D_{\infty h}$	2	2.99				1.04	
	Linear GaGaNNN (5D)	$C_{\infty v}$	2	2.97				1.22	
	Triangular bipyramidal (5E)	C_{2v}	2	2.66				2.62	
	Linear NGaGaNN (5F)	$C_{\infty v}$	2	2.29				1.44	
	Linear NGaNGaN (5G)	$D_{\infty h}$	4	1.92				1.06	
Ga_3N_2	Linear GaGaGaNN (6A)	$C_{\infty v}$	4	2.60	0.17	2.43		1.49	
	Rhomboidal planar (6B)	**C_{2v}**	**4**	**2.61**	**0.19**	**2.42**		**1.49**	
	Pentagonal (6C)	**C_{2v}**	**2**	**2.59**	**0.19**	**2.40**	4.59[d]	**2.28**	1.43[d]
	Planar (6D)	**C_{2v}**	**2**	**2.57**	**0.18**	**2.39**	4.54[d]	**2.69**	
	Linear GaNGaNGa (6E)	$D_{\infty h}$	**2**	2.37				1.74	
	Linear GaNNGaGa (6F)	$C_{\infty v}$	**2**	2.33				1.16	
	Triangular bipyramidal (6G)	D_{3h}	4	2.13				2.11	
	Linear GaNGaGaN (6H)	$C_{\infty v}$	**2**	1.98				2.11	
	Linear NGaGaGaN (6I)	$D_{\infty h}$	**2**	1.32				1.74	
Ga_4N	**Trapezoid (7A)**	**D_{4h}**	**2**	**2.23**	**0.10**	**2.13**	3.41[d] 2.43[b]	**1.53**	1.88[d] 0.63[b]
	Planar (7B)	**C_{2v}**	**2**	**2.19**	**0.13**	**2.06**	3.34[d]	**1.65**	
	Linear (GaGaGaNGa) (7C)	$C_{\infty v}$	**2**	1.84				1.18	
	Linear (GaGaNGaGa) (7D)	$D_{\infty h}$	**2**	1.83				0.68	
	Linear (GaGaGaGaN) (7E)	$C_{\infty v}$	**2**	1.15				0.90	

[a] Reference [21] (DFT-BPW91) (2003).
[b] Reference [28] (DMOL/GGA) (2006).
[c] Reference [16] (DMOL/GGA) (2000).
[d] Reference [26] (FP-LMTO) (2004).

N–N bond lengths are quite similar to their values. Our calculated bond angle NGaN of 72° is lower than the value of 95.2° given by Song and Cao [26]. No experimental data are available for comparison.

Ga_2N_3: We have studied seven configurations, as depicted in figure 5. Among them, four structures have high and comparable FBE. The two planar structures 5A and 5B have also been investigated earlier by Song *et al* [26, 42] who have reported very high BE as compared to ours. For both the structures 5A and 5B, the presently calculated Ga–Ga and Ga–N bond lengths are higher than those reported earlier [42].

Ga_3N_2: Nine different structures were investigated, as shown in figure 6. Four of them have high and similar FBE. The linear 6A structure has six imaginary frequencies (as shown later) and is thus unstable. Pentagonal (6C) and planar (6D) structures have also been investigated by

Table 2. Bond lengths (in Å) for all the most stable configurations of Ga_xN_y ($x + y = 2$–5) clusters.

			Bond lengths (Å)	
Cluster	Configuration	Bonds	Present	Others
GaN	Linear Ga–N (1A)	Ga–N	1.86	1.87[a,b], 1.88[c], 2.01[d], 2.06[e]
GaN_2	Linear GaNN (1B)	Ga–N	2.78	2.44[e], 2.32[f]
		N–N	1.10	1.14[e], 1.21[f]
	Triangular (1C)	Ga–N	3.25	2.58[e], 2.45[f], 2.24[g]
		N–N	1.10	1.16[e], 1.14[f], 1.15[g]
Ga_2N	Linear GaNGa (1E)	Ga–N	1.78	1.78[h,f], 1.79[a,e], 1.8[b]
GaN_3	Bent (2A)	N_1–N_2	1.14	1.14[a], 1.14[i]
		N_2–N_3	1.21	1.21[a], 1.21[i]
		N_3–Ga	1.92	1.93[a], 1.88[i]
Ga_2N_2	Rhombus (3C)	Ga–Ga	4.14	4.14[j], 4.21[e]
		Ga–N	2.16	2.16[j], 2.20[e]
		N–N	1.24	1.26[j], 1.27[e]
	Linear GaNNGa (3D)	Ga–N	1.97	2.00[j], 2.03[e]
		N–N	1.19	1.20[j], 1.21[e]
Ga_3N	Trigonal (3G)	Ga–N	1.91	1.94[b], 1.91[i], 1.92[g]
		Ga–Ga	3.32	3.32[b], 3.32[i], 3.32[g]
GaN_4	Bent-1 (4A)	Ga_1–N_2(N_4)	2.77	2.04[g]
		N_2–N_3	1.10	1.13[g]
		N_4–N_5	1.10	1.13[g]
Ga_2N_3	Planar-1 (5A)	Ga_1–Ga_2	2.96	2.74[i]
		Ga_1(Ga_2)–N_3	2.15	2.04[i]
		N_3–N_4	1.22	1.22[i]
		N_4–N_5	1.13	1.14[i]
	Planar-2 (5B)	Ga_1–Ga_2	3.43	3.15[i]
		Ga_1–N_5	2.23	2.10[i]
		Ga_2–N_3	2.23	2.10[i]
		N_3(N_5)–N_4	1.17	1.19[i]
		Ga_1(Ga_2)–N_4	2.79	
Ga_3N_2	Rhomboidal planar (6B)	Ga_2–Ga_1(Ga_3)	2.61	
		Ga_1–N_4	3.61	
		Ga_3–N_4	3.61	
		N_4–N_5	1.09	
	Pentagonal (6C)	Ga_1–Ga_2(Ga_5)	3.20	3.05[i]
		Ga_2–N_3	1.95	1.92[i]
		Ga_5–N_4	1.95	1.92[i]
		Ga_1–N_3(N_4)	2.23	2.16[i]
		N_3–N_4	1.24	1.26[i]
	Planar (6D)	Ga_1(Ga_3)–N_2	2.04	
		Ga_1(Ga_3)–N_4	2.25	
		Ga_5–N_4	1.91	
		N_2–N_4	1.33	
		Ga_1(Ga_3)–Ga_5	3.54	

Table 2. (Continued.)

Cluster	Configuration	Bonds	Bond lengths (Å) Present	Others
Ga_4N	Trapezoid (7A)	$Ga_2(Ga_3)$–N_1	2.03	
		$Ga_4(Ga_5)$–N_1	2.04	
		Ga_2–Ga_3	2.88	
		Ga_3–Ga_4	2.88	
		Ga_2–Ga_5	2.88	
		Ga_4–Ga_5	2.88	
	Planar (7B)	Ga_1–$Ga_2(Ga_3)$	2.89	
		Ga_2–Ga_3	2.96	
		$Ga_2(Ga_3)$–N_4	1.91	
		Ga_5–N_4	1.90	

[a] Reference [13] (B3LYP, BP86) (2000).
[b] Reference [28] (DMOL/GGA) (2006).
[c] Reference [41] (LCAO-MO) (2003).
[d] Reference [20] (DFT) (2000).
[e] Reference [16] (DMOL/GGA) (2000).
[f] Reference [27] (B3LYP, CCD) (2005).
[g] Reference [26] (FP-LMTO) (2004).
[h] Reference [15] (B3LYP) (2006).
[i] Reference [42] (FP-LMTO) (2004).
[j] Reference [21] (DFT-BPW91) (2003).

Song and Cao [26] whose BEs are seen to be about two times higher than ours. Our calculated various bond lengths are in general larger than those of Song *et al* [42] except the N–N bond length, where the reverse is true.

Ga_4N: Five different geometries, namely trapezoid, planar, and three linear chains (GaGaGaNGa, GaGaNGaGa and GaGaGaGaN) have been investigated, as shown in figure 7. All the structures have comparatively lower BEs as compare to the other five atom nanoclusters. The trapezoid (7A) and planar (7B) structures are seen to have quite similar FBEs. The 7A and 7B structures have also been found to be stable by Song and Cao [26]. On the other hand, only the structure 7A is found to be stable by Song *et al* [28]. Our BEs are much lower than those reported by earlier workers [26, 28].

The variation of the FBE with the cluster size ($x+y=n$) for the most stable configurations has been depicted in figure 8(a). We observe that the FBE increases quickly when one goes from $n=2$ to 3, and fluctuates thereafter. The most stable structures are those which contain the maximum number of nitrogen atoms because of the occurrence of strong N–N bonds. For the clusters containing one Ga, atom the FBE increases monotonically with the number of N atoms.

3.2. Electronic structure

The computed HOMO–LUMO gaps for all the studied structures are included in table 1, and their variation with the cluster size ($x+y=n$) for the most stable configurations has been depicted in figure 8(b). The HOMO–LUMO gap fluctuates with increase in the number of atoms. The nanoclusters containing odd (even) number of nitrogen atoms have large (small) HOMO–LUMO gap. The reported FPLMTO-MD HOMO–LUMO gaps are in general lower than the present values and other values obtained in other methods, except for GaN and Ga_4N (trapezoid) clusters.

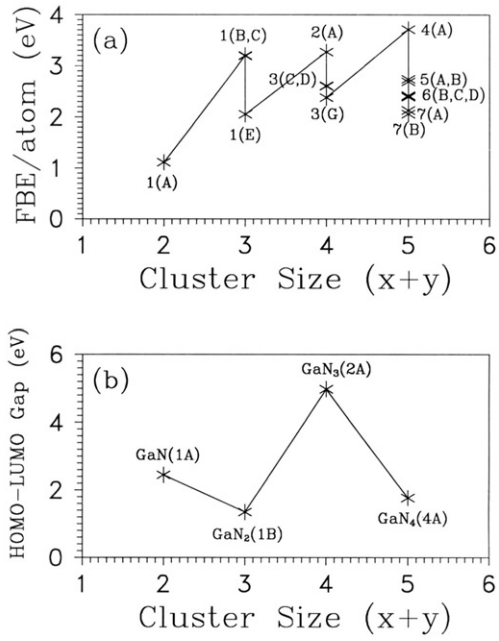

Figure 8. Variation of (a) final binding energy and (b) HOMO–LUMO gap with the cluster size $(x + y)$.

3.2.1. Ionization potential and electron affinity. The ionization potential (IP) is defined as the amount of energy required to remove an electron from a cluster. We determine the adiabatic IP by evaluating the energy difference between the neutral and the ionized clusters after finding the most stable state for the ionized clusters by using the optimization procedure. The adiabatic and vertical IPs and EAs for the most stable ones are included in table 3, which also includes the values calculated by others and the experimental values available for GaN clusters.

The electron affinity (EA) is defined as the energy released when an electron is added to a neutral cluster. We have determined the adiabatic EA by finding the energy difference between the neutral and the anionic clusters. The anionic cluster has been relaxed to its most stable state.

The charge on atoms of the most stable geometries of Ga_xN_y nanoclusters and their dipole moments are presented in table 4. The values of dipole moments reported by others are also depicted in table 4.

GaN: The present adiabatic IP is somewhat slightly smaller than the values of Kandalam *et al* [16], whereas the vertical IP is seen to lie in between the values reported by other workers [16, 28]. On the other hand, the present adiabatic EA is larger as compared to the other's value [21]. The present vertical EA is quite close to the values of Song *et al* [28] but smaller than the value given by Coastales and Pandey [21]. The present dipole moment for GaN molecule is larger than the value reported by Kandalam *et al* [16].

Ga_xN_y $(x + y = 3)$:

GaN_2: No other worker has computed IPs and EAs for this structure. The dipole moments of the two GaN_2 structures are quite small because of negligible charge transfer on the Ga and N atoms.

Table 3. Adiabatic and vertical ionization potential (IP) and electron affinity (EA) in eV for all the most stable configurations of Ga_xN_y ($x + y = 2$–5) clusters. The quantities given in brackets are the vertical IP and EA.

		IP (eV)		EA (eV)	
Cluster	Configuration	Present	Others	Present	Others
GaN	Linear Ga–N (1A)	8.103 (8.649)	8.24 (8.33)[a] (8.74)[b]	1.652 (1.539)	1.64 (1.77)[e] (1.51)[b]
GaN_2	Linear GaNN (1B)	5.842 (5.845)		0.506 (0.399)	
	Triangular (1C)	5.991 (5.995)		0.337 (0.331)	
Ga_2N	Linear GaNGa (1E)	8.082 (8.339)	7.98[c], (8.15)[b]	2.352[d] (2.348)	(2.0)[b]
GaN_3	Bent (2A)	9.022 (9.342)		0.285 (0.183)	
Ga_2N_2	Rhombus (3C)	6.025 (7.063)	6.26 (7.10)[a]	0.475 (0.138)	
	Linear GaNNGa (3D)	5.856 (6.535)		0.953 (0.884)	1.27 (1.74)[e]
Ga_3N	Trigonal (3G)	7.572 (7.734)	(7.28)[b]	0.590 (0.329)	(0.25)[b]
GaN_4	Bent-1 (4A)	5.689 (5.708)		0.303 (0.129)	
Ga_2N_3	Planar-1 (5A)	5.722 (6.203)		0.993 (0.853)	
	Planar-2 (5B)	5.108 (6.165)		1.122 (0.975)	
Ga_3N_2	Rhomboidal planar (6B)	6.152 (6.273)		1.620 (1.377)	
	Pentagonal (6C)	5.824 (6.757)		1.411 (1.227)	
	Planar (6D)	5.944 (6.834)		1.090 (0.722)	
Ga_4N	Trapezoid (7A)	6.601 (6.776)	(6.80)[b]	1.922 (1.884)	(1.74)[b]
	Planar (7B)	5.890 (6.072)		1.394 (1.289)	

[a] Reference [16] (DMOL/GGA) (2000).
[b] Reference [28] (DMOL/GGA) (2006).
[c] Reference [27] (B3LYP, CCD) (2005).
[d] Expt value = 2.51 eV [15].
[e] Reference [21] (DFT-BPW91) (2003).

Ga_2N: The present adiabatic IP is quite near the value reported by Wang and Balasubramanian [27], whereas our vertical IP is larger than the value of Song *et al* [28]. Our calculated adiabatic EA 2.35 eV is in good agreement with the experimental value of 2.51 [15]. Our predicted vertical EA is larger than the values reported by earlier workers [28]. The dipole moment is zero for Ga–N–Ga because of the symmetry of the structure.

Ga_xN_y ($x + y = 4$):

GaN_3: No earlier calculation is available for the IP and EA. There is large charge transfer between the various atoms which leads to the high dipole moment, 2.90 Debye.

Ga_2N_2: For the rhombus structure, Kandalam *et al* [16] have reported adiabatic and vertical IPs which are slightly higher than the present corresponding values. For linear GaNNGa, the adiabatic and vertical EAs reported by Coastales and Pandey [21] are much higher than the present values. The dipole moment for the rhombus and the linear GaNNGa is zero because of the symmetry consideration.

Ga_3N: Our values for vertical IP and EA are higher than those reported by Song *et al* [28]. Again, the symmetry of the structure leads to zero dipole moment.

Table 4. Charge on the atoms of the most stable configurations of Ga_xN_y ($x + y = 2$–5) clusters and their dipole moment (in Debye units). The charges are distributed on the atoms in the same order of atoms as given in table.

Cluster	Configuration	Charge on atoms					Dipole moment (Debye)
		q_1	q_2	q_3	q_4	q_5	Present
GaN	Linear NGa (1A)	−0.233	0.233				2.69[a]
GaN_2	Linear NNGa (1B)	0.182	−0.170	−0.012			0.11
	Triangular NGaN (1C)	0.002	−0.004	0.002			0.37
Ga_2N	Linear GaNGa (1E)	0.107	−0.214	0.107			0.00
GaN_3	Bent NNNGa (2A)	−0.053	0.226	−0.370	0.197		2.90
Ga_2N_2	Rhombus GaNGaN (3C)	0.217	−0.217	0.217	−0.217		0.00
	Linear GaNNGa (3D)	0.096	−0.096	−0.096	0.096		0.00
Ga_3N	Trigonal NGaGaGa (3G)	−0.295	0.099	0.098	0.098		0.003
GaN_4	Bent-1 GaNNNN (4A)	−0.022	−0.177	0.188	−0.177	0.188	0.14
Ga_2N_3	Planar-1 GaGaNNN (5A)	0.117	0.117	−0.439	0.196	0.009	1.58
	Planar-2 GaGaNNN (5B)	0.160	0.160	−0.351	0.382	−0.351	2.14
Ga_3N_2	Rhomboidal planar GaGaGaNN (6B)	0.023	−0.093	0.025	−0.152	0.197	0.66
	Pentagonal GaGaNNGa (6C)	0.298	0.031	−0.179	−0.179	0.029	0.81
	Planar GaNGaNGa (6D)	0.241	−0.168	0.241	−0.326	0.012	0.47
Ga_4N	Trapezoid NGaGaGaGa (7A)	−0.534	0.133	0.133	0.134	0.134	0.01
	Planar GaGaGaNGa (7B)	0.082	0.041	0.041	−0.263	0.099	1.13

[a] 2.04 Debye {Reference [16] (DMOL/GGA) (2000)}.

Ga_xN_y ($x + y = 5$):

GaN_4: The IPs and EAs have not been reported so far. Although there is large charge transfer between the N atoms, the dipole moment is quite small.

Ga_2N_3: Again, no earlier data either for IP or EA are available. The 5A structure has charge transfer larger than that of 5B, but both reveal appreciable dipole moment.

Ga_3N_2: No other worker has quoted the values of IP and EA. The dipole moments of 6B, 6C and 6D are small and quite similar.

Ga_4N: The vertical IP and EA calculated by Song *et al* [28] are quite similar to the present values. For structure 7A, the symmetry arguments will make the dipole moment zero. On the other hand, the 7B structure has appreciable dipole moment.

The variation of IP with the cluster size has been presented in figure 9(a). We observe that the IP shows a zigzag behaviour. The IPs for clusters containing an odd number of nitrogen atoms are greater than for clusters containing an even number of nitrogen atoms.

The variation of EA with the cluster size is shown in figure 9(b). The EA drops rapidly when the cluster size increases from $n = 2$ to 3, and shows slow fluctuations thereafter.

It may be pointed out that the adiabatic IP can be measured by using photoionization or photoelectron spectroscopic methods. On the other hand, when a technique such as fast electron bombardment is employed, the ionization occurs during the period of collision which enables the ionized cluster, and the IP is named as vertical. In general, in adiabatic IP and EA, the

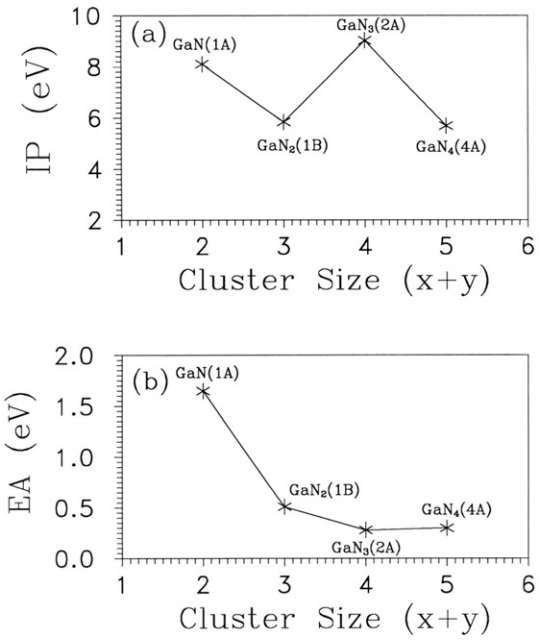

Figure 9. Variation of (a) adiabatic ionization potential and (b) adiabatic electron affinity with the cluster size $(x + y)$.

cationic and anionic cluster relaxes to the most stable ground state, whose energy is lower as compared to the ground state of the unrelaxed charged cluster. For the removal of an electron from the neutral cluster, one has to supply the necessary energy because the ground state of the cationic cluster is higher than the ground state of the neutral cluster by the same amount of energy, and this energy is called the IP. In the case of adiabatic ionization potential (AIP), the positively charged cluster relaxes by changing its atomic positions, acquiring various larger bond lengths to find a low-energy ground state as compared to the energy of the cationic cluster without any relaxation (used for the vertical IP). One observes dilation in the positively charged cluster because of the relaxation. The adiabatic IPs will thus be lower than the vertical IPs.

On the other hand, on adding an electron to the neutral cluster, the resulting ground state of the anionic cluster is lowered by an energy equal to the electron affinity. In this case, the anionic cluster is allowed to obtain the most stable ground state by incurring relaxation in the atomic positions. We find a contraction (smaller than the dilation observed in the cationic cluster) in the size of the cluster, reducing the various bond lengths. As a result of the atomic relaxation, the most stable ground state lies lower than the ground state corresponding to the unrelaxed cluster considered in determining the vertical EA. The adiabatic EAs are therefore larger than the vertical EAs.

3.3. Optical spectra and EELS

In figures 10–13, we present the calculated optical absorption spectra, which will be similar to the electron energy loss spectra (EELS). In most of the clusters, the absorption spectrum is quite weak in the visible region but is strong in the ultraviolet region. The excitation energies with the largest oscillator strengths for the most stable Ga_xN_y nanoclusters are given in table 5.

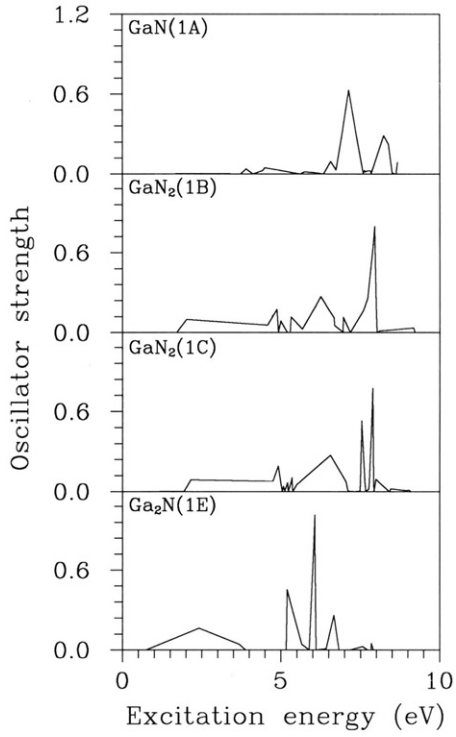

Figure 10. Absorption spectra for the most stable structures of GaN (1A), GaN_2, linear GaNN (1B) and triangular (1C) and Ga_2N, linear GaNGa (1E) nanoclusters.

Table 5. Excitation energies (ΔE, in eV) with largest oscillator strengths (f) for all the most stable configurations of Ga_xN_y ($x + y = 2$–5) clusters.

Cluster	Configuration	Excitation energy (ΔE, in eV)	Oscillator strength (f)
GaN	Linear Ga–N (1A)	7.13	0.63
GaN_2	Linear GaNN (1B)	7.95	0.80
	Triangular (1C)	7.89	0.78
Ga_2N	Linear GaNGa (1E)	6.07	1.01
GaN_3	Bent (2A)	7.77	0.64
Ga_2N_2	Rhombus (3C)	6.88	0.68
	Linear GaNNGa (3D)	7.19	0.69
Ga_3N	Trigonal (3G)	5.86	1.09
GaN_4	Bent-1 (4A)	7.89	0.73
Ga_2N_3	Planar-1 (5A)	7.80	0.55
	Planar-2 (5B)	7.55	0.68
Ga_3N_2	Rhomboidal planar (6B)	8.21	1.02
	Pentagonal (6C)	6.84	0.66
	Planar (6D)	6.49	0.49
Ga_4N	Trapezoid (7A)	6.23	0.81
	Planar (7B)	4.45	0.54

GaN: For the simplest diatomic molecule there is quite weak absorption in the energy region 3.7–6.7 eV. A very strong peak appears at 7.13 eV, and a doublet at 8.31 eV.

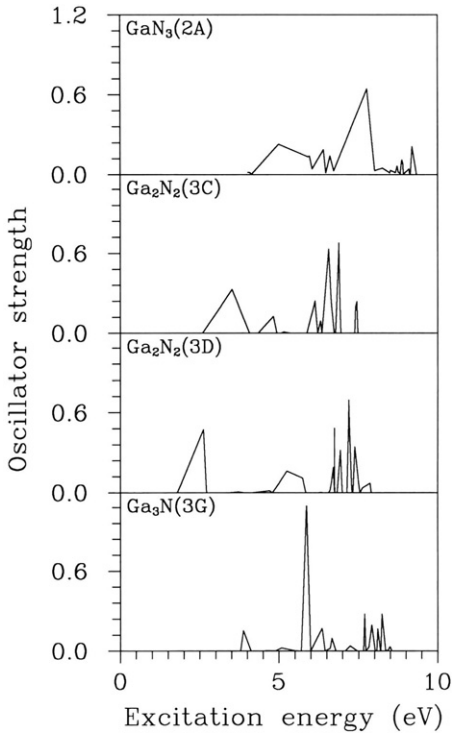

Figure 11. Absorption spectra for the most stable structures of GaN_3, bent (2A), Ga_2N_2, rhombus (3C) and linear GaNNGa (3D) and Ga_3N, trigonal (3G) nanoclusters.

Ga_xN_y ($x + y = 3$): For the two GaN_2 1B and 1C clusters, the absorption is quite similar, but there are some differences. The absorption starts at about 2.0 eV and is extended up to 8.0 or 9.0 eV for the 1B and 1C clusters, respectively. A strong peak at 7.95 eV appearing in the 1B cluster splits into two peaks occurring at 7.54 and 7.87 eV for the 1C structure.

For the triatomic Ga_2N cluster, there is weak absorption in the energy range 0.75–3.88 eV with a weak peak at 2.41 eV along with two strong peaks at 5.19 and 6.66 eV. A very strong peak also appears at 6.07 eV.

Ga_xN_y ($x + y = 4$): For the GaN_3 (2A) cluster, appreciable absorption starts at 4.0 eV and extends up to 9.3 eV, with a strong peak at 7.77 eV.

For the Ga_2N_2 (3C) cluster, the absorption is seen in the visible region. Strong peaks appear at 6.56 and 6.88 eV. On the other hand, for the Ga_2N_2 (3D) cluster configuration, the strong absorption appears at 2.61 eV, having a large width of 0.93 eV. A strong multiple peak absorption is seen in the region 6.7–7.5 eV.

For the Ga_3N (3G) cluster, the absorption is seen in the very high ultraviolet region, 5.7–8.5 eV, with a strong peak at 5.86 eV.

Ga_xN_y ($x + y = 5$): The optical spectrum of the GaN_4 (4A) cluster has weak absorption around 2.11 eV and also above 4.8 eV, but a strong peak appears at 7.89 eV.

The optical absorption spectrum of Ga_2N_3 (5A) shows weak peaks in the energy region 2.0–3.5 eV and also in 5.5–8.5 eV. One observes a strong peak at 7.80 eV. Also for the Ga_2N_3 (5B), one observes a sharp multipeak absorption spectrum in the energy region 2.0–8.0 eV.

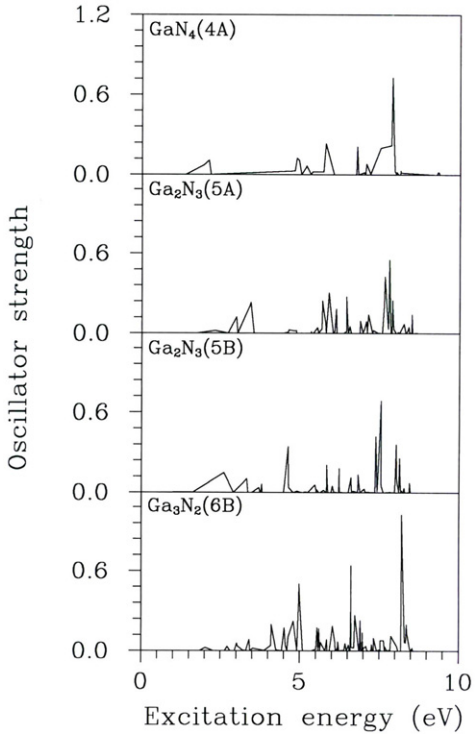

Figure 12. Absorption spectra for the most stable structures of GaN_4, bent-1 (4A), Ga_2N_3, planar-1 (5A) and planar-2 (5B) and Ga_3N_2, rhomboidal planar (6B) nanoclusters.

For the Ga_3N_2 (6B) cluster, multipeak absorption is seen, starting from 2.0 to 8.5 eV. Strong and sharp peaks appear at 4.98, 6.60 and 8.21 eV. For the Ga_3N_2 (6C) cluster, the absorption is seen in the energy range 1.3–7.8 eV, with strong peaks at 3.79 and 6.84 eV. Also, for the Ga_3N_2 (6D) cluster, a sharp multipeak spectrum is seen in the energy range 2.0–8.0 eV.

The optical absorption spectrum of Ga_4N (7A) commences at about 2.9 eV and extends up to 7.4 eV. A strong and sharp peak appears at 6.23 eV. For Ga_4N (7B), a sharp multipeak structure is observed in the approximate energy range of 4.0–7.2 eV.

3.4. Vibrational frequencies

The vibrational frequencies are calculated using the B3LYP-DFT/6-311G(3df) method for the most stable nanoclusters. We calculate the second derivative of total energy of the system with respect to the atomic displacements. The obtained dynamical matrix is diagonalized. We have also calculated the infrared intensities (IR Int.), relative infrared intensities (Rel. IR Int.) and Raman scattering activities (Raman activity). The above calculated physical quantities for the two-atom and three-atom clusters are presented in table 6, for four-atom clusters in table 7 and for five-atom clusters in table 8, respectively. In these tables, the brackets following the frequencies contain the multiplicity of the mode. We discuss each nanocluster below.

GaN: We obtain the stretching mode frequency of 593 cm^{-1}, which is 20% higher than the measured [13] value of 485 cm^{-1}, and a similar high frequency has been obtained by earlier workers [13, 21, 28], except by Kandalam *et al* [16], who have reported a frequency

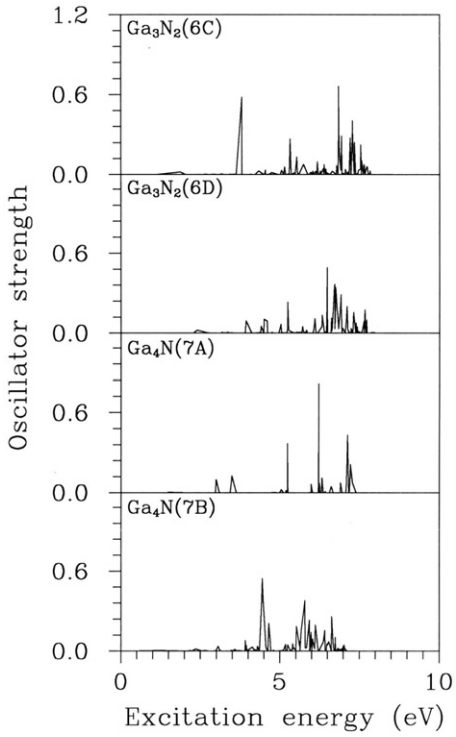

Figure 13. Absorption spectra for the most stable structures of Ga_3N_2, pentagonal (6C) and planar (6D) and Ga_4N, trapezoid (7A) and planar (7B) nanoclusters.

of 447 cm^{-1}, lower than the experimental value. This stretching frequency is both IR and Raman active. Our calculated IR intensity is in close agreement with others [13].

Ga_xN_y ($x + y = 3$):

GaN_2: For the linear GaNN (1B) structure, we obtained the stretching frequency of the closely spaced N–N atom at 2342 cm^{-1}. On the other hand, the Ga–N stretching frequency is quite low (44 cm^{-1}) because of the large separation between the Ga and the centre of mass of the two N atoms. The two other low frequencies, 55 and 88 cm^{-1}, are the transverse frequencies belonging to the displacements of the atoms normal to the linear chain.

For the triangular (1C) structure, we obtain three frequencies. The highest one (2360 cm^{-1}) arises from the stretching vibration of the N–N bond. The low frequencies originate from the stretching vibration of Ga–N bond, etc. Our N–N frequency is higher than the earlier reported value. For both the 1B and 1C structures, the highest stretching frequencies are both highly IR and Raman active. No experimental data are available for comparison.

Ga_2N: For the linear GaNGa symmetric structure, the calculated frequencies are 892, 304, and the doubly degenerate 46 cm^{-1}. The highest frequency of 892 cm^{-1} corresponds to the Ga–N stretching vibration. The frequency 304 cm^{-1} arises from the breathing motion of the two outermost Ga atoms. The remaining low frequency belongs to the atomic displacement normal to the linear chain. Our calculated stretching frequency is 18% higher than the experimental

Table 6. Ga_xN_y ($x + y = 2, 3$) clusters: the calculated vibrational frequencies (cm^{-1}), infrared intensities (IR Int. in km mol^{-1}), relative IR intensities (Rel. IR Int.) and Raman scattering activities (Raman activity in A^4/amu). Brackets following the frequencies contain the multiplicity of the mode.

Configuration		Properties	Values
Linear Ga–N (1A)	Present	Frequency	593
		IR Int.	17.74
		Rel. IR Int.	1.0
		Raman activity	78 028.79
	Expt.	Frequency	485[a]
	Others	Frequency	581[a], 597[a], 591[b], 595[c], 447[d]
		IR Int.	24[a], 18[a]
Linear GaNN (1B)	Present	Frequencies	44, 53, 88, 2342
		IR Int.	1.11, 0.11, 0.01, 519.60
		Rel. IR Int.	0.0, 0.0, 0.0, 1.0
		Raman activity	16.59, 0.00, 1.17, 6538.03
Triangular GaN_2 (1C)	Present	Frequencies	30, 113, 2360
		IR Int.	1.25, 0.98, 288.85
		Rel. IR Int.	0.00, 0.00, 1.0
		Raman activity	9.30, 9.93, 4120.32
	Others	Frequencies[f]	127, 275, 1968
Linear GaNGa (1E)	Present	Frequencies	46 (2), 304, 892
		IR Int.	23.92, 0.0, 3.64
		Rel. IR Int.	1.0, 0.0, 0.15
		Raman activity	0.0, 3.04, 0.0
	Expt.	Frequencies[a]	757.4
		Frequencies[e]	345 ± 40, 740 ± 40
	Others	Frequencies[f]	87 (2), 302, 889
		Frequencies[f]	53 (2), 331, 830
		Frequencies[e]	51 (2), 301, 878
		Frequencies[a]	64 (2), 297, 867
		IR Int.[a]	32, 0.0, 4.0
		Frequencies[a]	54 (2), 295, 868
		IR Int.[a]	27, 0.0, 20

[a] Reference [13] (B3LYP, BP86) (2000).
[b] Reference [28] (DMOL/GGA) (2006).
[c] Reference [21] (DFT-BPW91) (2003).
[d] Reference [16] (DMOL/GGA) (2000).
[e] Reference [15] (B3LYP) (2006).
[f] Reference [27] (B3LYP, CCD) (2005).

value. Similar values have also been reported by earlier workers. On the other hand, the present breathing mode frequency of 304 cm^{-1} is lower than the experimental value of 345 ± 40 cm^{-1}. The IR Int. values reported by other workers are quite near to the present ones.

Ga_xN_y ($x + y = 4$):

GaN_3: For the bent (2A) structure, the two highest frequencies are again higher than experimental values, by about 6–7%. Others have reported computed values similar to ours. Our predicted IR Int. are also in agreement with the earlier values. The linear GaNNN (2B) structure possesses one imaginary frequency and therefore is unstable.

Table 7. Ga_xN_y ($x + y = 4$) clusters: the calculated vibrational frequencies (cm^{-1}), infrared intensities (IR Int. in km mol^{-1}), relative IR intensities (Rel. IR Int.) and Raman scattering activities (Raman activity in A^4/amu). Brackets following the frequencies contain the multiplicity of the mode.

Configuration		Properties	Values
Bent (2A)	Present	Frequencies	71, 398, 609, 619, 1402, 2243
		IR Int.	0.38, 121.49, 11.02, 14.84, 244.34, 944.48
		Rel. IR Int.	0.0, 0.13, 0.01, 0.02, 0.26, 1.0
		Raman activity	3.67, 17.55, 0.01, 0.11, 15.46, 88.84
	Expt.	Frequencies[a]	1328, 2096
	Others	Frequencies[a]	58, 384, 595, 598, 1408, 2231
		IR Int.[a]	1.0, 133, 15, 16, 249, 1080
Linear GaNNN (2B)	Present	Frequencies	54i (2), 367, 605(2), 1440, 2254
		IR Int.	2.06, 119.84, 13.69, 291.26, 895.70
		Rel. IR Int.	0.00, 0.13, 0.02, 0.33, 1.0
		Raman activity	5.56, 22.61, 0.01, 12.53, 82.85
Tetrahedral Ga_2N_2 (3A)	Present	Frequencies	26i, 20, 28, 39, 157, 2424
		IR Int.	0.0, 0.01, 0.15, 0.11, 0.04, 18.51
		Rel. IR Int.	0.0, 0.0, 0.01, 0.01, 0.0, 1.0
		Raman activity	1.37, 12.60, 0.94, 7.20, 78.28, 788.72
Linear GaGaNN (3B)	Present	Frequencies	68i (2), 12 (2), 35, 200, 2450
		IR Int.	68.14, 0.43, 0.30, 0.01, 0.45
		Rel. IR Int.	1.0, 0.01, 0.0, 0.0, 0.01
		Raman activity	4.57, 76.02, 890.70, 23 303.77, 354.79
Rhombus Ga_2N_2 (3C)	Present	Frequencies	118, 139, 180, 456, 483, 1492
		IR Int.	2.34, 25.86, 0.0, 331.47, 0.0, 0.0
		Rel. IR Int.	0.01, 0.08, 0.0, 1.0, 0.0, 0.0
		Raman activity	0.0, 0.0, 136.39, 0.0, 25.40, 625.88
	Others	Frequencies[a]	135, 151, 179, 453, 463, 1492
		IR Int.[a]	3, 27, 0, 328, 0, 0
		Frequencies[b]	154, 165, 174, 426, 456, 1372
		Rel. IR Int.[b]	0.09, 0.0, 0.01, 1.0, 0.0, 0.0
Linear GaNNGa (3D)	Present	Frequencies	53 (2), 192 (2), 197, 492, 1689
		IR Int.	3.57, 0.0, 0.0, 389.67, 0.0
		Rel. IR Int.	0.01, 0.0, 0.0, 1.0, 0.0
		Raman activity	0.0, 46.43, 408.56, 0.0, 10 476.43
	Others	Frequencies[a]	70 (2), 182, 209, 455, 1687
		IR Int.[a]	5, 0.0, 0.0, 388, 0.0
		Frequencies[c]	89, 193, 383, 489, 1739
Trigonal Ga_3N (3G)	Present	Frequencies	96.7, 97.2, 180, 256, 647, 648
		IR Int.	0.87, 0.83, 1.39, 0.0, 396.46, 396.43
		Rel. IR Int.	0.0, 0.0, 0.0, 0.0, 1.0, 0.99
		Raman activity	6.68, 6.70, 0.0, 36.13, 3.16, 3.16
	Others	Frequencies[a]	96.9, 97.1, 183, 256, 640, 653
		IR Int.[a]	1.0, 1.0, 3.0, 0.0, 399.0, 402.0
		Frequencies[a]	92 (2), 169, 249, 631 (2)
		IR Int.[a]	1.0, 3.0, 0.0, 362

[a] Reference [13] (B3LYP, BP86) (2000).
[b] Reference [16] (DMOL/GGA) (2000).
[c] Reference [21] (DFT-BPW91) (2003).

Table 8. Ga_xN_y ($x + y = 5$) clusters: the calculated vibrational frequencies (cm^{-1}), infrared intensities (IR Int. in km mol^{-1}), relative IR intensities (Rel. IR Int.) and Raman scattering activities (Raman activity in A^4/amu). Brackets following the frequencies contain the multiplicity of the mode.

Configuration	Properties	Values
Bent-1 GaN_4 (4A)	Frequencies	33, 47, 52, 71, 97, 110, 111, 2335, 2355
	IR Int.	0.07, 1.16, 0.44, 0.0, 0.01, 0.0, 0.01, 468.32, 420.40
	Rel. IR Int.	0.0, 0.0, 0.0, 0.0, 0.0, 0.0, 0.0, 1.0, 0.90
	Raman activity	10.99, 18.30, 5.07, 4.03, 0.93, 2.62, 12.39, 7166.40, 4500.68
Planar-1 Ga_2N_3 (5A)	Frequencies	78, 94, 105, 255, 262, 613, 631, 1326, 2218
	IR Int.	2.22, 0.07, 2.54, 55.03, 9.07, 7.50, 0.13, 270.23, 1028.09
	Rel. IR Int.	0.00, 0.0, 0.0, 0.05, 0.01, 0.01, 0.0, 0.26, 1.0
	Raman activity	10.91, 3.08, 50.05, 12.29, 0.00, 0.04, 0.01, 46.81, 144.91
Planar-2 Ga_2N_3 (5B)	Frequencies	75, 86, 145, 199, 273, 633, 639, 1362, 2087
	IR Int.	0.98, 0.0, 7.26, 1.81, 75.14, 16.72, 2.25, 0.08, 400.55
	Rel. IR Int.	0.0, 0.0, 0.02, 0.01, 0.19, 0.04, 0.01, 0.0, 1.0
	Raman activity	81.76, 0.34, 1.68, 7.11, 3.31, 18.17, 0.07, 19.25, 8.93
Linear GaGaGaNN (6A)	Frequencies	19i (2) 16i (2) 4i (2), 17, 132, 219, 2451
	IR Int.	0.01, 0.16, 0.00, 0.06, 0.04, 62.68, 0.08
	Rel. IR Int.	0.0, 0.0, 0.0, 0.0, 0.0, 1.0, 0.0
	Raman activity	4.26, 2.40, 11.89, 0.09, 175.31, 0.0, 58.02
Rhomboidal planar Ga_3N_2 (6B)	Frequencies	15, 23, 32, 49, 61, 75, 169, 173, 2437
	IR Int.	0.40, 0.01, 0.01, 0.16, 0.36, 0.69, 7.32, 0.64, 12.03
	Rel. IR Int.	0.0, 0.0, 0.0, 0.01, 0.03, 0.06, 0.61, 0.05, 1.0
	Raman activity	2.10, 2.15, 3.03, 2.93, 30.93, 0.52, 9.49, 88.52, 766.55
Pentagonal Ga_3N_2 (6C)	Frequencies	52, 55, 82, 180, 203, 283, 297, 516, 1440
	IR Int.	1.73, 2.41, 1.36, 0.0, 9.25, 57.87, 18.31, 468.55, 21.77
	Rel. IR Int.	0.0, 0.01, 0.0, 0.0, 0.02, 0.12, 0.04, 1.0, 0.05
	Raman activity	0.05, 2.79, 1.15, 31.18, 70.77, 217.35, 57.51, 0.07, 2409.28
Planar Ga_3N_2 (6D)	Frequencies	40, 65, 81, 158, 197, 255, 410, 536, 1157
	IR Int.	0.01, 1.35, 3.42, 2.78, 16.21, 103.65, 178.69, 279.14, 14.78
	Rel. IR Int.	0.0, 0.01, 0.01, 0.01, 0.06, 0.37, 0.64, 1.0, 0.05
	Raman activity	4.55, 0.05, 5.82, 1.89, 57.10, 3.20, 38.11, 0.11, 312.91
Trapezoid Ga_4N (7A)	Frequencies	28, 61, 62, 121.6, 122.4, 182, 212, 430.7, 431
	IR Int.	0.0, 0.07, 0.07, 0.0, 0.0, 0.46, 0.0, 181.35, 181.96
	Rel. IR Int.	0.0, 0.0, 0.0, 0.0, 0.0, 0.0, 0.0, 0.99, 1.0
	Raman activity	0.0, 0.0, 0.0, 22.58, 1.31, 0.0, 89.55, 0.0, 0.0
Planar Ga_4N (7B)	Frequencies	29, 49, 89, 107, 134, 154, 259, 485, 746
	IR Int.	0.08, 0.01, 2.07, 2.22, 3.23, 5.50, 4.81, 3.25, 673.20
	Rel. IR Int.	0.0, 0.0, 0.00, 0.00, 0.01, 0.01, 0.01, 0.01, 1.0
	Raman activity	2.54, 2.46, 14.83, 18.94, 6.22, 4.24, 34.77, 87.79, 17.23

Ga_2N_2: The tetrahedral (3A) and linear GaGaNN (3B) structures which show an imaginary frequency are unstable.

For the rhombus (3C), there are six frequencies. The highest frequency (1492 cm^{-1}) originates from the breathing of the two N atoms. The next lower frequency, 483 cm^{-1}, belongs to the shear motion of the N atoms. The remaining four frequencies originate from the mixed vibration of the Ga and N atoms. The B3LYP calculation performed by Zhou and Andrews [13]

has reported theoretical values slightly different from ours and shows the case for the IR Int. It may be noted that the present method employes the basis 6-311G(3df) in contrast to the basis 6-311 + G^* considering the diffuse function that is used by Zhou and Andrews [13]. On the other hand, Kandalam *et al* [16] have obtained four highest frequencies lower than the present values.

The linear structure GaNNGa (3D) has seven frequencies in all. The highest frequency, 1689 cm^{-1}, is for the N–N stretching vibration. Zhou and Andrews [13] have obtained similar frequencies and IR Int. after using the B3LYP method. Costales and Pandey [21] have obtained frequencies higher as compared to ours and others.

Ga_3N: The trigonal (3G) structure has low vibrational frequencies because of the occurrence of Ga–N bonds. There are two doubly degenerate modes possessing either the highest frequency (647, 648 cm^{-1}) or the lowest frequency (96.7, 97.2 cm^{-1}). The earlier results of Zhou and Andrews [13] using the B3LYP method are quite similar to present values.

Ga_xN_y ($x + y = 5$):

GaN_4: For the bent-1 structure (4A), the upper two frequencies (2355 and 2335 cm^{-1}) are associated with the stretching vibrations of the N atoms close to the Ga atom.

Ga_2N_3: For the planar structures 5A and 5B, the highest frequencies (2218 and 2087 cm^{-1}) belong to stretching vibration of the two ends of the chain of the N atoms. The next vibration (1326 cm^{-1}) originates from the stretching vibration of the two inner atoms, but here the two outer atoms move in the same direction. The next low frequencies (631 and 613 cm^{-1}, etc) correspond to the vibrations where N atoms move normal to the N–N–N chain.

Ga_3N_2: For the rhomboidal planar structure (6B), the N–N stretching vibration has the frequency 2437 cm^{-1}. The lower frequencies correspond to either transverse N–N or Ga–N stretching modes.

For the pentagonal structure (6C), the N–N stretching frequency turns out to be 1440 cm^{-1}. For the planar structure (6D), the N–N stretching frequency reduces to 1157 cm^{-1} because of the attached Ga atoms.

Ga_4N: For the trapezoid structure (7A), the two high (431, 430.7 cm^{-1}) vibrations belong to the symmetric and asymmetric stretching vibrations of the constituent Ga–N–Ga configuration.

For the planar structure (7B), the highest frequency (746 cm^{-1}) originates from the stretching vibration of the Ga–N tail. The other ones belong to different symmetric vibrations of Ga atoms.

The above study of the various vibrations of the different structures shows that the high vibration frequencies lying in the range 431–2437 cm^{-1} arise from the stretching vibrations of the N–N bonds. The lower frequencies belong either to the Ga–N stretching vibration or the bending vibrations. Our calculated frequencies are in general 6–20% higher than the experimental data. However, the theoretical values reported by earlier workers are quite similar to ours. The discrepancy may be attributed to the neglect of the role of anharmonicity.

In the above discussion, we find that, although three of the linear chains, namely GaNNN (2B), GaGaNN (3B), GaGaGaNN (6A), and the tetrahedral Ga_2N_2 (3A) structures have high BEs, their lower frequencies are seen to be imaginary, which will result in their instability.

4. Conclusion

The present study establishes the occurrence of the most stable configurations of the various Ga_xN_y nanoclusters. For Ga_xN_y nanoclusters, we have predicted the bond lengths, binding energies, HOMO–LUMO gaps, adiabatic and vertical ionization potentials and electron affinities, charge on atoms, dipole moments, vibrational frequencies, IR Int., Rel IR Int. and Raman scattering activities, some of which need to be verified experimentally. The results are, in general, in good agreement with the experimental data wherever available.

The most stable structures are those which contain the maximum number of nitrogen atoms because of the occurrence of the strongest N–N bonds, whereas the lowest binding is seen for clusters containing the maximum number of gallium atoms because of the occurrence of the maximum number of the weak Ga–Ga bonds. For the clusters containing the maximum number of nitrogen atoms i.e. clusters containing only one gallium atom, the BE increases monotonically with the number of nitrogen atoms.

In all the studied nanoclusters, the FPLMTO-MD values for the BEs are much higher than those of the present study and those of other workers using other methods. Our values for the various structures are also lower than the values reported by other workers using other methods.

The HOMO–LUMO gap fluctuates with increase in the number of atoms. The clusters containing odd (even) number of nitrogen atoms have large (small) HOMO–LUMO gap. The reported FPLMTO-MD HOMO–LUMO gaps are, in general, lower than the present and others values, except for the GaN and Ga_4N (trapezoid) clusters.

In general, the adiabatic IP (EA) is smaller (greater) than the vertical IP (EA) because of the lower energies of the most stable ground state of the cationic (anionic) clusters.

The optical absorption spectrum, or EELS, has been computed for each most stable cluster. The spectrum is unique for every cluster and may be used to characterize a specific cluster.

The present study of the vibrational frequencies of the various structures shows that the high vibration frequencies lying in the range 431–2437 cm^{-1} originate from the stretching vibrations of the N–N bonds. The lower frequencies belong to either Ga–N stretching vibrations or bending vibrations. Our calculated frequencies are, in general, 6–20% higher than the experimental data. However, the theoretical values reported by earlier workers are quite similar to ours. The discrepancy may be attributed to the neglect of the role of anharmonicity.

We find that, although three linear chains, namely GaNNN (2B), GaGaNN (3B), GaGaGaNN (6A), and the tetrahedral Ga_2N_2 (3A) structures have high BEs, as their low frequencies are imaginary, they may not be stable.

Acknowledgment

The authors are thankful to University Grants Commissions and Defence Research and Development Organisation, New Delhi, for financial assistance.

References

[1] Perlin P, Gorczyca I, Christensen N E, Gizegory I, Teisseyre M and Suski T 1992 *Phys. Rev.* B **45** 13307
[2] Ponce F A and Bour D P 1997 *Nature* **27** 351
Normile D 1997 *Science* **275** 1734
[3] Nakamura S 1996 *Proc. Int. Symp. on Blue Laser and Light Emitting Diodes* ed A Yoshikawa, K Kishino, M Kobayashi and T Yasuda (Japan: Chiba University Press) p 119
[4] Jena P, Rao B K and Khanna S N 1990 *Physics and Chemistry of Small Clusters* (*NATO ASI Series* vol 158) (Dordrecht: Kluwer)

[5] Bernstein E R (ed) 1990 Atomic and molecular clusters *Studies in Physical and Theoretical Chemistry* vol 68 (Amsterdam: Elsevier)
[6] Jarrold M F 1991 *Science* **252** 1085
[7] Hartke B 2002 *Angew. Chem. Int. Edn Engl.* **41** 1468
[8] Mattei G 2002 *Nucl. Instrum. Methods Phys. Res.* B **191** 323
[9] McMurran J, Dai D, Balasubramanian K, Steffek C, Kouvetakis J and Hubbard J L 1998 *Inorg. Chem.* **37** 6638
[10] Huang Y, Duan X F, Cui Y and Lieber C M 2002 *Nano Lett.* **2** 101
[11] Johnson J C, Choi H J, Knutsen K P, Schaller R D, Yang P D and Saykally R J 2002 *Nat. Mater.* **1** 106
[12] Ervin K M and Lineberger W C 1992 *Advances in Gas Phase Ion Chemistry* vol 1, ed N G Adams and L M Babcock (London: JAI Press) pp 121–66
[13] Zhou M and Andrews L 2000 *J. Phys. Chem.* A **104** 1648
[14] Himmel H J and Hebben N 2005 *Chem. Eur. J.* **11** 4096
[15] Sheehan S M, Meloni G, Parsons B F, Wehres N and Neumark D M 2006 *J. Chem. Phys.* **124** 064303
[16] Kandalam A K, Pandey R, Blanco M A, Costales A, Recio J M and Newsam J M 2000 *J. Phys. Chem.* B **104** 4361
[17] Kandalam A K, Blanco M A and Pandey R 2001 *J. Phys. Chem.* B **105** 6080
[18] Kandalam A K, Blanco M A and Pandey R 2002 *J. Phys. Chem.* B **106** 1945
[19] Costales A, Blanco M A, Pendas A M, Kandalam A K and Pandey R 2002 *J. Am. Chem. Soc.* **124** 4116
[20] BelBruno J J 2000 *Heteroat. Chem.* **11** 281
[21] Costales A and Pandey R 2003 *J. Phys. Chem.* A **107** 191
[22] Song B and Cao P L 2002 *Phys. Lett.* A **300** 485
[23] Song B and Cao P L 2003 *Chin. Phys. Lett.* **20** 1488
[24] Song B and Cao P L 2002 *Phys. Lett.* A **306** 57
[25] Song B, Cao P L and Li B X 2003 *Phys. Lett.* A **315** 308
[26] Song B and Cao P L 2004 *Phys. Lett.* A **328** 364
[27] Wang C S and Balasubramanian K 2005 *Chem. Phys. Lett.* **402** 294
[28] Song B, Yao C H and Cao P L 2006 *Phys. Rev.* B **74** 035306
[29] Burke K, Petersilka M and Gross E K U 2002 *Recent Advances in Density Functional Methods* vol III, ed P Fantucci and A Bencini (Singapore: World Scientific) p 67
[30] Rubio A, Alonso J A, Blase X and Balbas L C 1996 *Phys. Rev. Lett.* **77** 247
[31] Vasiliev I, Ogut S and Chelikowsky J R 1999 *Phys. Rev. Lett.* **82** 1919
[32] Vasiliev I, Ogut S and Chelikowsky J R 2002 *Phys. Rev.* B **65** 115416
[33] Stratmann R E, Scuseria G E and Frisch M J 1998 *J. Chem. Phys.* **109** 8218
[34] Bauernschmitt R and Ahlrichs R 1996 *Chem. Phys. Lett.* **256** 454
[35] Casida M E, Jamorski C, Casida K C and Salahub D R 1998 *J. Chem. Phys.* **109** 4439
[36] Becke A D 1993 *J. Chem. Phys.* **98** 5648
Becke A D 1988 *Phys. Rev.* A **38** 3098
[37] Lee C, Yang W and Parr R G 1988 *Phys. Rev.* B **37** 785
[38] Miehlich B, Savin A, Stoll H and Preuss H 1989 *Chem. Phys. Lett.* **157** 200
[39] Gaussian, Inc. 2003 *GAUSSIAN 03, Revision C.03* (Pittsburgh, PA: Gaussian)
[40] Lide D R (ed) 1989–90 *CRC Handbook of Chemistry and Physics* 70th edn (Boca Raton, FL: CRC Press) p F-189, 199–200
[41] Das G P, Rao B K and Jena P 2003 *Phys. Rev.* B **68** 035207
[42] Song B, Ling L and Cao P L 2004 *Chin. Phys.* **13** 489